ACS Editors' Choice

JACS
JOURNAL OF THE AMERICAN CHEMICAL SOCIETY

Communication

pubs.acs.org/JACS

Terms of Use

Polyethylenimine-Enhanced Electrocatalytic Reduction of CO_2 to Formate at Nitrogen-Doped Carbon Nanomaterials

Sheng Zhang,[†] Peng Kang,[†] Stephen Ubnoske,[‡] M. Kyle Brennaman,[†] Na Song,[†] Ralph L. House,[†] Jeffrey T. Glass,[‡] and Thomas J. Meyer*[,†]

[†]Department of Chemistry, University of North Carolina at Chapel Hill, Chapel Hill, North Carolina 27599, United States
[‡]Department of Electrical and Computer Engineering, Duke University, Durham, North Carolina 27708, United States

Supporting Information

ABSTRACT: Nitrogen-doped carbon nanotubes are selective and robust electrocatalysts for CO_2 reduction to formate in aqueous media without the use of a metal catalyst. Polyethylenimine (PEI) functions as a co-catalyst by significantly reducing catalytic overpotential and increasing current density and efficiency. The co-catalysis appears to help in stabilizing the singly reduced intermediate $CO_2^{\bullet-}$ and concentrating CO_2 in the PEI overlayer.

Accumulation of carbon dioxide in the atmosphere is considered a major contributor to climate change through global warming.[1] Once captured, CO_2 is a potentially useful feedstock if it can be converted into formate/formic acid, carbon monoxide, or more highly reduced hydrocarbon products. Electrochemical and photoelectrochemical CO_2 reduction could become an integral part of an energy storage strategy with solar- or wind-generated electricity used to store energy in the chemical bonds of carbon-based fuels. Electrochemical reduction of CO_2 has yet to be achieved on appropriately large scales due, in part, to the lack of efficient, robust catalysts operating at low overpotentials with high selectivities and current densities.

Most studies on CO_2 reduction catalysis have used noble metal Au, Ir, and Ag catalysts,[2] with extensions to base metals (Cu, Sn, etc.)[3] and their oxides.[4] Only a limited effort has been devoted to carbon-based materials,[5] conducting polymers,[6] and nonmetallic homogeneous catalysts.[7] Nitrogen-doped carbon materials are notable as electrode choices due to their low cost and high surface areas, and significant electrocatalytic activity has been described.[8] These materials have also been used for both electrochemical oxygen reduction[9] and water oxidation,[10] with performances comparable to those of metal-based catalysts. Recently, N-doped carbon nanofibers were reported for CO_2 reduction to CO in ionic liquids.[5a] The work of Bocarsly on pyridine/pyridinium catalytically reducing CO_2 to methanol and other reduced carbon products is especially notable.[7a,d,e]

Inspired by the initial results on N-containing materials, we report here results of an ammonia plasma study on N-doping of carbon nanotubes (CNT). N-doping initiates electrocatalytic reduction of CO_2 to formate in aqueous solutions. We also report on a co-catalytic effect by an overlayer film of polyethylenimine (PEI), a polymer with amine functional groups that is commonly used as a CO_2 absorbent.[11] The combination of N-doping of CNT and use of a PEI overlayer leads to a significant reduction in overpotential and enhanced Faradaic efficiencies and current densities for CO_2 reduction to formate in water. Formate, or its protonated form, formic acid, is used as a preservative and antibacterial agent in livestock feed, a coagulant in the production of rubber, a hydrogen storage material, and the anode fuel in direct formic acid fuel cells.[12]

Scheme 1. Fabrication of Nitrogen-Doped Carbon Nanotubes on Glassy Carbon Electrodes with an Overlayer of Polyethylenimine (PEI-NCNT/GC)

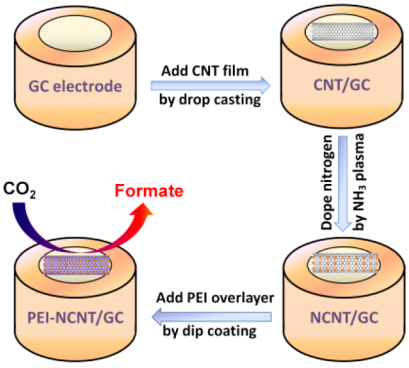

As shown in Scheme 1, multiwalled CNT were first dispersed in dimethylformamide by sonication to yield a homogeneous CNT suspension that was drop-cast onto a prepolished glassy carbon (GC) electrode. Nitrogen-doped carbon nanotubes (NCNT) were synthesized by exposing the CNT/GC electrodes to an ammonia plasma. The plasma treatment is a facile, room-temperature doping method, with the dopant content varied by changing plasma power intensities, chamber pressures, and exposure times.[13] In the present study, the extent of N-doping was controlled by varying exposure time, with the results, monitored by X-ray photoelectron spectroscopy (XPS) analysis (Figures 1a and S1), shown in Table S1. From these results, the nitrogen content in the doped CNT first increased with exposure time, leveling off after 40 min of exposure to give the NCNT-coated glassy carbon electrodes (NCNT/GC) used in subsequent electrochemical experiments.

Oxygen-doped carbon nanotubes on glassy carbon (OCNT/GC) were prepared by using a similar procedure but with use of

Received: March 28, 2014
Published: April 29, 2014

   dx.doi.org/10.1021/ja5031529 | J. Am. Chem. Soc. 2014, 136, 7845−7848

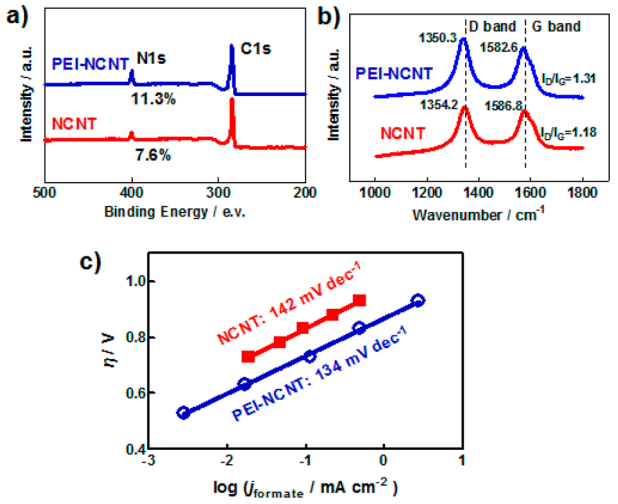

Figure 1. (a) XPS and (b) Raman spectra. (c) Formate partial current density Tafel plots at NCNT and PEI-NCNT. Data for the Tafel plot were obtained in 0.1 M $KHCO_3$/CO_2-saturated water.

an oxygen plasma. Physical characterization (Figures S1 and S2) confirmed the doping of nitrogen and oxygen into the CNT. The plasma treatment provided a reliable method for obtaining consistent dopant concentrations in the CNT electrodes. Quantitative comparisons of the impact on reactivity toward CO_2 reduction to formate for are presented among the various stages of electrode evolution are presented below.

Prior to electrochemical measurements, the doped electrodes were subjected to an additional electrochemical purification step (see Supporting Information (SI)) to remove residual Fe particles within the CNT. After purification, there was no residual peak for elemental Fe by high-resolution XPS analysis (note Figure S3). The electroactive surface areas of the electrodes were evaluated by cyclic voltammetry with the ferri-/ferrocyanide couple ($[Fe(CN)_6]^{3-/4-}$) used as the reference probe (see Figure S4). The results of these experiments showed an increase in surface area following the ammonia and oxygen plasma treatments. The increase can be attributed to the fact that the surface layer of the CNT was partially etched away by the plasma during the N- or O-doping, allowing accessibility of inner carbon layers to the external solution.[14]

Electrocatalytic CO_2 reduction by CNT/GC, NCNT/GC, and OCNT/GC electrodes was evaluated by controlled potential electrolyses in 0.1 M $KHCO_3$ solutions saturated with CO_2 (Tables 1, S1, and S2). The products of CO_2 reduction were analyzed by both ^{1}H NMR for the liquid phase and gas chromatography for the headspace. Formate, H_2, and trace

Table 1. Current Densities (j) and Faradaic Efficiencies for Formate ($F_{formate}$) Following Production Controlled Potential Electrolyses at −1.8 V vs SCE in 0.1 M $KHCO_3$/CO_2 Aqueous Solution at Various Electrodes

	electrodes					
	CNT	OCNT	NCNT	PEI-CNT	PEI-NCNT	PEI-NGCNT
$j_{geometric}$ (mA/cm^2)	1.3	3.6	3.0	3.8	7.2	9.5
$j_{electroactive}$ (mA/cm^2)	0.6	1.4	1.3	1.3	2.2	3.8
$F_{formate}$ (%)	5	7	59	8	85	87

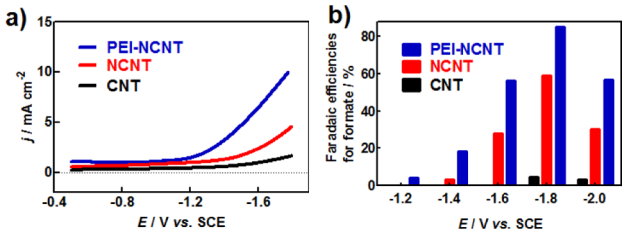

Figure 2. (a) Cathodic linear sweep voltammetry scans at 50 mV/s in a CO_2-saturated aqueous 0.1 M $KHCO_3$ solution. (b) Plot of Faradaic efficiencies for formate production vs applied potential at CNT/GC, NCNT/GC, and PEI-NCNT/GC electrodes.

amounts of CO were produced during the electrolyses. Both NCNT and OCNT electrodes exhibited 2-fold higher current densities (over 3 mA/cm^2) relative to CNT (1.3 mA/cm^2), but the reduction products differed significantly. Optimized NCNT electrodes demonstrated significantly higher Faradaic efficiencies for formate (59%) than either OCNT (7%) or CNT (5%), with 39% H_2 and 2% CO also formed. OCNT and CNT electrodes mainly gave H_2 as the product (>90%) with a small amount of CO (<1%). Maximum Faradaic efficiencies for formate were achieved by using NCNT electrodes with a nitrogen content of >7 atom%; further N-doping provided no further improvement. Higher doping levels may decrease the electrical conductivity of the NCNT electrodes. These results suggest that N-doping plays a nontrivial role in CO_2 reduction to formate.

PEI (see Figure S5 for structure) has a high adsorption capacity and selectivity toward CO_2 adsorption. In aqueous solutions it is positively charged because of partial protonation at the amine N's with pK_a = 7−9 under neutral pH conditions in the external solution.[15] It can be attached to the surfaces of CNT through non-covalent dispersion interactions based on van der Waals forces,[16] driven largely by elimination of the hydrophobic interface between the CNT and water.

In our experiments, a PEI overlayer was applied to NCNT/GC electrodes by dip-coating followed by rinsing with excess water to obtain PEI-NCNT/GC electrodes. Based on the XPS spectra in Figure 1a, the nitrogen content was increased from 7.6 at.% in NCNT to 11.3 at.% at the PEI-NCNT interface, demonstrating the presence of PEI at the surfaces of the CNT in ∼17 mass% (see SI for details of the evaluation). Raman spectra (Figure 1b) show that PEI functionalization of the nanotube surfaces results in a slight increase in the intensity ratio of the D band over the G band, consistent with a slightly more disordered nanotube structure. A decrease in peak position of ∼4 cm^{-1} was also observed, suggesting that charge transfer from the electron-donating PEI to CNT induces slightly more disorder in the underlying CNT structure. This observation is also consistent with reports of PEI used as an electron donor to modify CNT.[9b]

PEI functionalization reduced catalytic overpotential and enhanced both Faradaic efficiencies and current densities for formate production. As shown in Figure 2a, PEI-NCNT exhibited a more positive onset potential than the other two electrodes. Figure 3c shows the result of a controlled potential electrolysis of a PEI-NCNT/GC electrode at −1.8 V for 24 h, which resulted in a steady-state catalytic current density of 7.2 mA/cm^2, comparable to that obtained with Sn catalysts (1−10 mA/cm^2)[3b,4a] evaluated in a three-compartment electrochemical cell. The appearance of sustained currents shows that the PEI overlayer is stable on the surface of NCNT.

Formate was shown to be the dominant electrolysis product at PEI-NCNT/GC electrodes. It was formed in 85% yield and

dx.doi.org/10.1021/ja5031529 | J. Am. Chem. Soc. 2014, 136, 7845−7848

detected directly by *in situ* electrochemical Raman monitoring (see Figure S6 for details). As shown in Figure 2b, the Faradaic efficiency for formate at PEI-NCNT/GC electrodes reaches a maximum at −1.8 V and decreases at more negative potentials due to an increase in competing background H_2 evolution.[3b]

Current densities normalized for electroactive surface area in Table 1 were 2.2 mA/cm^2 for PEI-NCNT and 1.3 mA/cm^2 for NCNT. Reduction at −1.2 V (an overpotential of 0.54 V for CO_2 reduction with E^o = −0.66 V vs SCE for the CO_2/$HCOO^-$ couple at pH 6.8) produced formate in 4% yield at PEI-NCNT. By contrast, the onset potentials for CO_2 reduction to formate were ca. −1.8 V for CNT and −1.4 V for NCNT. These results suggest that PEI functions as a co-catalyst in promoting CO_2 reduction at NCNT.

Tafel plots for CO_2 reduction are shown in Figure 1c. From these data, Tafel slopes were 142 and 134 mV/dec for NCNT/GC and PEI-NCNT/GC electrodes, respectively (Figure S7). Both values are close to the 118 mV/dec expected for rate-limiting single-electron transfer at the electrode. Transfer coefficients (α) were 0.42 and 0.44 at NCNT/GC and PEI-NCNT/GC. Exchange current densities, i_0, were ∼1.4 × 10^{-7} and 4.6 × 10^{-7} mA/cm^2 for NCNT and PEI-NCNT, respectively. The i_0 value is about 3-fold higher for PEI-NCNT than for NCNT. It is also larger than the i_0 value at Hg (1.5 × 10^{-9} mA/cm^2) and approaches i_0 for Sn (1.2 × 10^{-6} mA/cm^2),[17] in both cases for CO_2 reduction to formate. The magnitude of i_0 reflects the free energy barrier to CO_2 reduction at the reversible potential and is a measure of the intrinsic catalytic activities of electrode materials and interfaces.[18]

From the comparisons presented here, the intrinsic catalytic activity of PEI-NCNT is comparable to that of the best metal electrodes for CO_2 reduction to formate.

Graphenated carbon nanotubes (GCNT) were utilized to further increase catalytic current density. With its unique three-dimensional (3D) nanostructure, GCNT has shown promise as an electrocatalytic substrate.[8d] It has the advantage of high electrical conductivity and offers both the high surface area framework of CNT and the high edge density and reactivity of graphene nanosheets. In our studies, GCNT was prepared by chemical vapor deposition, resulting in graphene foliates along the length of aligned CNT (see ref 19 for details of the synthesis), and then transferred onto GC electrodes (GCNT/GC, see SI for details). N-doped NGCNT/GC and PEI-NGCNT/GC electrodes were obtained by using the procedure in Scheme 1.

Figure 3a,b depicts SEM cross-sectional images of a typical film (with ∼20 μm thick films shown in Figure S8) of aligned CNT with graphene foliates along their length, at different resolutions. XPS (Figure S9) and Raman spectra (Figure S10) were used to demonstrate adsorption of PEI on the surface of NGCNT. Electrolyses at PEI-NGCNT/GC electrodes (Figure 3c) were conducted at −1.8 V for 24 h in CO_2-saturated 0.1 M $KHCO_3$ aqueous solution. The Faradaic efficiency for formate production at PEI-NGCNT/GC was 87%, comparable to that found for PEI-NCNT. The geometric current density was increased to 9.5 mA/cm^2, and the catalytic current density, normalized for electroactive surface area (Figure S11), of 3.8 mA/cm^2 was higher than for PEI-NCNT. The rate enhancement can be attributed to higher edge densities and CO_2 transport rates for the 3D GCNT compared to conventional CNT. The results summarized in Tables 1 and S2 also confirm that PEI functionalization significantly improves performance toward electrocatalytic CO_2 reduction at N-doped, 3D GCNT.

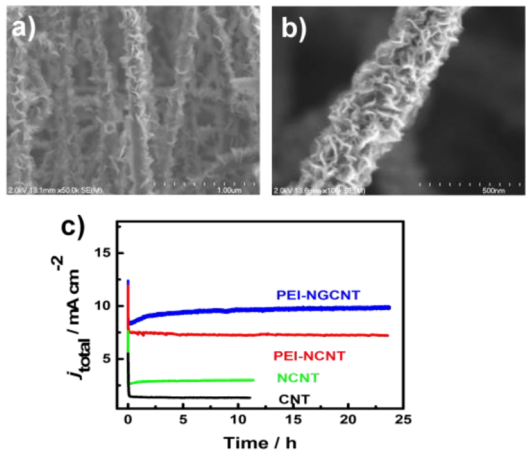

Figure 3. (a,b) Cross-sectional SEM images of GCNT. (c) Controlled potential electrolyses at −1.8 V vs SCE at various electrodes in 0.1 M $KHCO_3$/CO_2-saturated water. j_{total} is the geometric current density.

The co-catalytic role of PEI is a notable finding. It significantly improves performance toward CO_2 reduction, but only with N-doped carbon nanomaterials. PEI-functionalized, but undoped, PEI-CNT electrodes did not exhibit obvious improvements over CNT electrodes (Table 1). This points to a concerted interaction between PEI and the NCNT interface in a rate-limiting step or steps in the catalytic reduction of CO_2 that is absent with a PEI overlayer on pristine CNT.

The results of the Tafel analysis of the data in Figure 1c point to rate-determining electron transfer to CO_2 to give the $CO_2^{\bullet-}$ anion radical. The thermodynamic potential for CO_2 reduction to $CO_2^{\bullet-}$ is −2.21 V vs SCE, compared to −0.67 V vs SCE for 2e$^-$ reduction to $HCOO^-$ at pH 7. With N-doping, the single-electron reduction onset shifts anodically to −1.4 V at NCNT (Figure 2), a net 400 mV decrease in overpotential compared to CNT.

From the high-resolution N 1s XPS spectra of NCNT in Figure S12, pyridinic-N (62.5%) and pyrrolic-N (23.7%) are the dominant nitrogen sites. In both, the N atoms are polarized negatively due to electron-withdrawing effects in the graphene π system, with the adjacent C atoms polarized positively.[9a,20] In the proposed mechanism in Scheme 2, CO_2 is presumably first adsorbed to the basic nitrogen binding sites[7a] in NCNT, where it is reduced to $CO_2^{\bullet-}$. The PEI overlayer may stabilize $CO_2^{\bullet-}$ by a H-bond interaction, NCNT−N−C(O)O$^{\bullet-}$···H−N−PEI, thus

Scheme 2. Proposed Mechanism for CO_2 Reduction at PEI-Functionalized, Nitrogen-Doped Carbon Nanomaterials

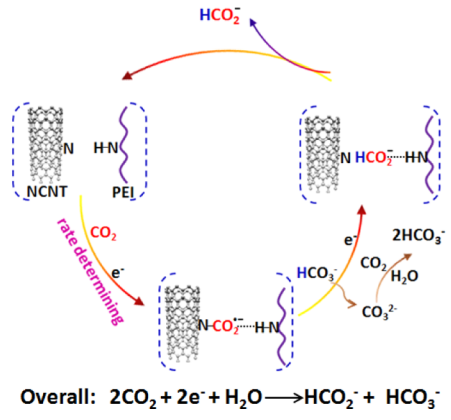

dx.doi.org/10.1021/ja5031529 | J. Am. Chem. Soc. 2014, 136, 7845−7848

lowering the onset potential for reducing CO_2 to $CO_2^{\bullet-}$ by creating a stabilizing environment. This hypothesis is supported by the fact that the overpotential for CO_2 reduction to formate is further reduced by 200 mV after addition of the PEI overlayer to NCNT. In addition, given its known ability to adsorb CO_2, the adsorbed PEI overlayer may concentrate CO_2 on the electrode surface from the bulk solution, increasing its effective local concentration.

In the mechanism in Scheme 2, once formed, the stabilized CO_2 radical is protonated and further reduced, with the probable proton source being HCO_3^-, given its smaller pK_a (10.33) compared to that of H_2O (15.7). Protonated PEI and carbonic acid are present in the CO_2-saturated solutions but in kinetically insignificant amounts. Protonation is followed by, or occurs in concert with, a rapid, second electron-transfer reduction to give formate as the product.

In summary, ammonia plasma treatment with N-doping followed by adsorption of PEI has been used to create a facile and efficient local environment for selective reduction of CO_2 to formate on carbon surfaces. The plasma treatment results in the doping of high surface area carbon nanomaterials with nitrogen, with notable enhancements in performance toward electrocatalytic CO_2 reduction to formate. The combination of N-doping and a PEI overlayer has a synergistic effect, creating a local environment in which reduction of CO_2 to $CO_2^{\bullet-}$ occurs at a greatly reduced overpotential. The decrease in overpotential is accompanied by corresponding enhancements in Faradaic efficiency and current density for formate production.

In CO_2-saturated aqueous $KHCO_3$ solutions, maximum Faradaic efficiencies for formate production of 87% have been reached with current densities of 9.5 mA/cm^2 on 3D GCNT. The resulting catalytic electrodes are highly stable in extended controlled potential electrolyses. The optimized metal-free electrodes show overall performances on par with those of the most efficacious metal electrodes, and their fabrication is straightforward.

The results of this study may open a new avenue for highly efficient CO_2 reduction catalysis based on inexpensive, easily prepared carbon-based materials and inspire application of related co-catalysis strategies to other reactions of interest.

■ ASSOCIATED CONTENT

Ⓢ Supporting Information

Materials preparation, electrochemical measurements, and physical characterizations. This material is available free of charge via the Internet at http://pubs.acs.org.

■ AUTHOR INFORMATION

Corresponding Author

tjmeyer@unc.edu

Notes

The authors declare no competing financial interest.

■ ACKNOWLEDGMENTS

This research was supported primarily by the UNC EFRC Center for Solar Fuels, an Energy Frontier Research Center funded by the U.S. Department of Energy Office of Science, Office of Basic Energy Sciences, under award no. DE-SC0001011, supporting S.Z., P.K., M.K.B., N.S., and R.L.H. We acknowledge funding from National Science Foundation, contract DMR-1106173, supporting S.U. We thank Drs. Carrie Donley and Amar Kumbhar (CHANL) for assistance with XPS and SEM measurements.

■ REFERENCES

(1) Karl, T. R.; Trenberth, K. E. *Science* **2003**, *302*, 1719.

(2) (a) Rosen, B. A.; Salehi-Khojin, A.; Thorson, M. R.; Zhu, W.; Whipple, D. T.; Kenis, P. J. A.; Masel, R. I. *Science* **2011**, *334*, 643. (b) Lu, Q.; Rosen, J.; Zhou, Y.; Hutchings, G. S.; Kimmel, Y. C.; Chen, J. G.; Jiao, F. *Nat. Commun.* **2014**, *5*, 3242. (c) Kang, P.; Cheng, C.; Chen, Z.; Schauer, C. K.; Meyer, T. J.; Brookhart, M. *J. Am. Chem. Soc.* **2012**, *134*, 5500. (d) Kang, P.; Meyer, T. J.; Brookhart, M. *Chem. Sci.* **2013**, *4*, 3497.

(3) (a) Kuhl, K. P.; Cave, E. R.; Abram, D. N.; Jaramillo, T. F. *Energy Environ. Sci.* **2012**, *5*, 7050. (b) Zhang, S.; Kang, P.; Meyer, T. J. *J. Am. Chem. Soc.* **2014**, *136*, 1734. (c) Wu, J. J.; Risalvato, F. G.; Ke, F. S.; Pellechia, P. J.; Zhou, X. D. *J. Electrochem. Soc.* **2012**, *159*, F353. (d) DiMeglio, J. L.; Rosenthal, J. *J. Am. Chem. Soc.* **2013**, *135*, 8798. (e) Hori, Y.; Wakebe, H.; Tsukamoto, T.; Koga, O. *Electrochim. Acta* **1994**, *39*, 1833. (f) Costentin, C.; Drouet, S.; Robert, M.; Savéant, J.-M. *Science* **2012**, *338*, 90.

(4) (a) Chen, Y.; Kanan, M. W. *J. Am. Chem. Soc.* **2012**, *134*, 1986. (b) Li, C. W.; Kanan, M. W. *J. Am. Chem. Soc.* **2012**, *134*, 7231. (c) Le, M.; Ren, M.; Zhang, Z.; Sprunger, P. T.; Kurtz, R. L.; Flake, J. C. *J. Electrochem. Soc.* **2011**, *158*, E45.

(5) (a) Kumar, B.; Asadi, M.; Pisasale, D.; Sinha-Ray, S.; Rosen, B. A.; Haasch, R.; Abiade, J.; Yarin, A. L.; Salehi-Khojin, A. *Nat. Commun.* **2013**, *4*, 2819. (b) Nakata, K.; Ozaki, T.; Terashima, C.; Fujishima, A.; Einaga, Y. *Angew. Chem., Int. Ed.* **2014**, *53*, 871.

(6) Aydin, R.; Koleli, F. *J. Electroanal. Chem.* **2002**, *535*, 107.

(7) (a) Barton Cole, E.; Lakkaraju, P. S.; Rampulla, D. M.; Morris, A. J.; Abelev, E.; Bocarsly, A. B. *J. Am. Chem. Soc.* **2010**, *132*, 11539. (b) Riduan, S. N.; Zhang, Y.; Ying, J. Y. *Angew. Chem., Int. Ed.* **2009**, *48*, 3322. (c) Seshadri, G.; Lin, C.; Bocarsly, A. B. *J. Electroanal. Chem.* **1994**, *372*, 145. (d) Yan, Y.; Zeitler, E. L.; Gu, J.; Hu, Y.; Bocarsly, A. B. *J. Am. Chem. Soc.* **2013**, *135*, 14020. (e) Morris, A. J.; McGibbon, R. T.; Bocarsly, A. B. *ChemSusChem* **2011**, *4*, 191.

(8) (a) Tornow, C. E.; Thorson, M. R.; Ma, S.; Gewirth, A. A.; Kenis, P. J. A. *J. Am. Chem. Soc.* **2012**, *134*, 19520. (b) Zheng, Y.; Jiao, Y.; Chen, J.; Liu, J.; Liang, J.; Du, A.; Zhang, W.; Zhu, Z.; Smith, S. C.; Jaroniec, M.; Lu, G. Q.; Qiao, S. Z. *J. Am. Chem. Soc.* **2011**, *133*, 20116. (c) Liu, R. L.; Wu, D. Q.; Feng, X. L.; Mullen, K. *Angew. Chem., Int. Ed.* **2010**, *49*, 2565. (d) Li, Y. G.; Zhou, W.; Wang, H. L.; Xie, L. M.; Liang, Y. Y.; Wei, F.; Idrobo, J. C.; Pennycook, S. J.; Dai, H. J. *Nat. Nanotechol.* **2012**, *7*, 394.

(9) (a) Gong, K. P.; Du, F.; Xia, Z. H.; Durstock, M.; Dai, L. M. *Science* **2009**, *323*, 760. (b) Wang, S.; Yu, D.; Dai, L. *J. Am. Chem. Soc.* **2011**, *133*, 5182.

(10) Zhao, Y.; Nakamura, R.; Kamiya, K.; Nakanishi, S.; Hashimoto, K. *Nat. Commun.* **2013**, *4*, 2390.

(11) Sanz, R.; Calleja, G.; Arencibia, A.; Sanz-Perez, E. S. *J. Mater. Chem. A* **2013**, *1*, 1956.

(12) Zhang, S.; Shao, Y.; Yin, G.; Lin, Y. *Angew. Chem., Int. Ed.* **2010**, *49*, 2211.

(13) Shao, Y. Y.; Zhang, S.; Engelhard, M. H.; Li, G. S.; Shao, G. C.; Wang, Y.; Liu, J.; Aksay, I. A.; Lin, Y. H. *J. Mater. Chem.* **2010**, *20*, 7491.

(14) Jiao, L.; Zhang, L.; Ding, L.; Liu, J.; Dai, H. *Nano Res.* **2010**, *3*, 387.

(15) Kozlovskaya, V.; Kharlampieva, E.; Drachuk, I.; Cheng, D.; Tsukruk, V. V. *Soft Matter* **2010**, *6*, 3596.

(16) Tasis, D.; Tagmatarchis, N.; Bianco, A.; Prato, M. *Chem. Rev.* **2006**, *106*, 1105.

(17) (a) Ryu, J.; Andersen, T. N.; Eyring, H. *J. Phys. Chem.* **1972**, *76*, 3278. (b) Prakash, G. K. S.; Viva, F. A.; Olah, G. A. *J. Power Sources* **2013**, *223*, 68.

(18) Gileadi, E. *Electrode Kinetics for Chemists, Chemical Engineers and Materials Scientists*; Wiley: Weinheim, 1993.

(19) Parker, C. B.; Raut, A. S.; Brown, B.; Stoner, B. R.; Glass, J. T. *J. Mater. Sci.* **2012**, *27*, 1046.

(20) Kim, H.; Lee, K.; Woo, S. I.; Jung, Y. *Phys. Chem. Chem. Phys.* **2011**, *13*, 17505.